J Bionic Eng 15 (2018) 941–949
DOI: https://doi.org/10.1007/s42235-018-0082-0

Journal of Bionic Engineering
http://www.springer.com/journal/42235

Parametric Gait Online Generation of a Lower-limb Exoskeleton for Individuals with Paraplegia

Tianjiao Zheng[1], Yanhe Zhu[1*], Zongwei Zhang[1], Sikai Zhao[1], Jie Chen[2], Jie Zhao[1]

1. *State Key Laboratory of Robotics and System*, *Harbin Institute of Technology*, *Harbin* 150001, *China*
2. *School of Mechanical Engineering and Automation*, *Northeastern University*, *Shenyang* 110819, *China*

Abstract

Lower-limb exoskeletons can provide paraplegics with the ability to restore gait function. In the community ambulation, the user would frequently meet different floors, doorsills, and other obstacles. Therefore, parametric gait generation is a significant issue for this kind of exoskeletons. In this paper, a parametric gait online generation approach is proposed, which combines a parametric gait control method with a torque compensation control strategy, based on the state machine. In the torque compensation control, the reference trajectories of joint positions are obtained through compensating gravity, inertia, and friction, which is intent on the natural and well-directed source data. Based on the reference trajectories, the parametric gait control method is established, in which the gait can be controlled *via* three parameters: velocity, step-length, and step-height. Two test cases are performed on three healthy subjects. The results demonstrate that the parametric gait can be online generated smoothly and correctly, meanwhile every variable step can be triggered as users expect. The effectiveness and practicability of the gait generation approach proposed in this paper are validated. In addition, this research is the foundation of autonomous gait planning.

Keywords: exoskeleton, parametric gait, gait online generation, paraplegic, bionic design

1 Introduction

There are numerous persons suffering physical disabilities, because of stroke, Spinal Cord Injury (SCI), trauma, bone tuberculosis, and other diseases. Only owing to SCI, there are over millions people with paraplegia around the world. Besides loss of mobility, paraplegia could also lead to a series of complications, including bedsore, osteoporosis, bowel/bladder dysfunction, mental health problems, life expectancy, and economic burden[1–3].

In order to restore some degree of legged mobility and mitigate the secondary injuries to individuals with paraplegia, lower-limb exoskeleton as an effective mean is a focused topic in recent years[4–12]. Lower-limb exoskeleton which is a kind of wearable robots could provide the paraplegics with the ability to upright walk through supplying and maintaining the strength of bilateral lower-limbs.

A number of lower-limb exoskeletons for impaired populations have been developed and described in the scientific literatures. Moreover, several exoskeletons for paraplegics are commercially available, such as Rewalk™ (ReWalk Robotics Ltd., Israel, rewalk.com)[13,14], Ekso™ (Ekso Bionics Ltd., USA, eksobionics.com)[15,16], Indego™ (Parker Hannifin Corp., USA, www.indego.com)[17–21], and HAL® (Cyberdyne Inc., Japan, www.cyberdyne.jp)[22–25].

The additional locomotion function, walking, is the dominant goal for the paraplegia patients. Therefore, design, generation, and control of gait are the significant issues for the exoskeleton developments. Based on the state machine, gait is usually divided into finite modes which can be triggered by button, sensors, or other external devices[13–17,19–21,23]. Position-based control is more likely to be used to assist paraplegics' locomotion to apply a set of predefined joint angle trajectories in the modes[4]. These predefined trajectories can be adjusted offline as requirements[13–15,19,20,22,26]. In addition, the source data of these predefined trajectories are obtained mostly by motion capture devices and Clinical Gait Analysis (CGA) database. The parametric gait is more useful and effective for the community ambulation, in which the user frequently meets different floors, door-

***Corresponding author:** Yanhe Zhu
E-mail: yhzhu@hit.edu.cn

sills, and other obstacles[27,28]. Whereas, the parametric gait of exoskeletons is rare in the literatures.

The goal of this research is to establish a natural and convenient gait generation method of lower-limb exoskeleton for paraplegics. With this method, the gait based on references can be online generated through adjusting the predefined parameters as users expect. Moreover, the source data of references are natural, well-directed, and reliable. Furthermore, this method is employed and tested on a novel exoskeleton, which is developed with modular structure and steel cable transmission system.

In this paper, design and development of our exoskeleton are specified first, followed by the description of parametric gait online generation in the third section. Tests and results are presented in the fourth section. The conclusions are given in the final section.

2 Exoskeleton design and development

2.1 Mechanism design

Fig. 1 shows a lower-limb exoskeleton for individuals with paraplegia, which is designed by our research group at Harbin Institute of Technology (HIT, China). The user of this exoskeleton is expected to have sufficient upper body strength to maintain balance with a walker or forearm crutches. This exoskeleton has five components: waist, bilateral thighs, and bilateral shanks. The bilateral joints of hip and knee are actuated in the sagittal plane. The motion ranges of these joints are comparable to those of a healthy individual (hip: −30° – 120°, knee: 0° – 120°). In addition, the first prototype has a weight of 10.15 kg.

The entire systems of motor, actuator, and transmission for hip and knee joints are laid on the bilateral thighs symmetrically. The speed reduction ratio of each joint transmission system is selected to 510: 1, where 51: 1 comes from the planetary gearbox, 2: 1 comes from a pair of bevel gears, and 5: 1 comes from the steel cable transmission, as shown in Fig. 2. Brushless DC motor (Maxon EC-4Pole30, 100 W) through transmission system enables each joint to provide up to 20.6 N·m of torque continuously and 96.0 N·m of torque instantaneously. Meanwhile, the continuous speed of each joint is 33 rpm.

Fig. 1 HIT lower-limb exoskeleton for individuals with paraplegia.

2.2 Control system architecture

The control system architecture serves two functions: (a) to obtain the position, velocity, acceleration, and current signals which are needed for control and data acquisition; (b) to generate the power signal to activate the motors. As shown in Fig. 3, our lower-limb exoskeleton has a three-layer control system architecture, which includes distributed embedded system (driver, motor, and sensor), main controller, and host PC.

The main controller is designed based on DSP (TMS320F28335) and ARM (STM32F103). The communication between the main controller and the distributed embedded system is based on CANOpen protocol wired CAN bus. The motor is driven by utilizing the Elmo driver. A novel absolute magnetic encoder is specially designed and employed to assist the position detection. In addition, a handle is specially designed to remotely manipulate the exoskeleton, which is based on the STM32 and wirelessly communicated with the main controller by means of ZigBee.

3 Parametric gait online generation

3.1 Idea and framework

Based on the state machine, authors combine two kinds of control methods to achieve the effective gait of the exoskeleton. In order to obtain the reference position

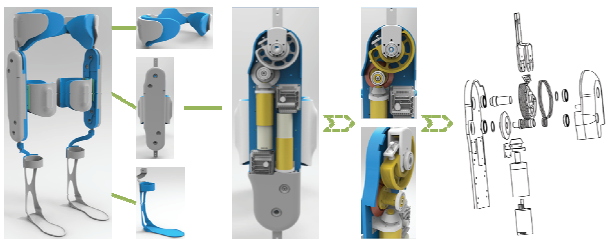

Fig. 2 The structure of transmission system.

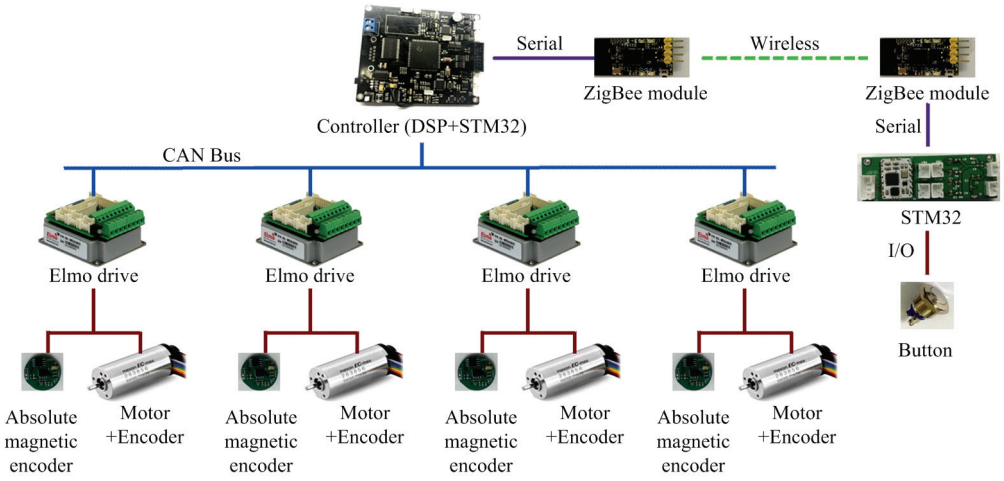

Fig. 3 The control system architecture.

data of the joint motions, a torque compensation control strategy is designed, in which gravity, inertia, and friction are compensated. Meanwhile, a parametric gait online control method based on the references is proposed. As shown in Fig. 4, this state machine has four basic states, which are seated, double-support stance, left foot stepping and right foot stepping. Transitions between these basic states are realized by typical motions, which are triggered by the handle.

In this research, the exoskeleton itself is a detection device utilizing the above method. With this approach, the errors due to different conditions between detection and execution devices can be eliminated as much as possible. The motion data are reliable and well-directed from the source.

3.2 Data acquisition and procession

In the process of data acquisition, the exoskeleton employs the torque compensation control, which compensates its gravity, inertia, and friction. As a result, the reverse drivability of the exoskeleton is improved significantly. The exoskeleton can follow the user's movements effortlessly. Therefore, more accurate data can be detected and gathered.

The dynamic equation of the exoskeleton is:

$$\boldsymbol{H}(\boldsymbol{\theta})\ddot{\boldsymbol{\theta}} + \boldsymbol{C}(\boldsymbol{\theta},\dot{\boldsymbol{\theta}})\dot{\boldsymbol{\theta}} + \boldsymbol{F}\dot{\boldsymbol{\theta}} + \boldsymbol{G}(\boldsymbol{\theta}) = \boldsymbol{T}_e, \tag{1}$$

where $\boldsymbol{\theta}$ is the vector of exoskeleton joint angles, $\boldsymbol{H}(\boldsymbol{\theta})$ is the inertial matrix, $\boldsymbol{C}(\boldsymbol{\theta},\dot{\boldsymbol{\theta}})$ is Coriolis force matrix, $\boldsymbol{F}$ is the friction coefficient matrix, $\boldsymbol{G}(\boldsymbol{\theta})$ is the gravitational torque matrix, and $\boldsymbol{T}_e$ is the vector of joint torques actuated by motors.

Design the feed forward control law as:

$$\hat{\boldsymbol{T}}_e = \hat{\boldsymbol{H}}(\boldsymbol{\theta})\ddot{\boldsymbol{\theta}} - \boldsymbol{K}_D\dot{\boldsymbol{\theta}} + \hat{\boldsymbol{F}}\dot{\boldsymbol{\theta}} + \hat{\boldsymbol{G}}(\boldsymbol{\theta}), \tag{2}$$

where $\hat{\boldsymbol{T}}_e$ is the vector of compensation torques actuated by motors, $\boldsymbol{K}_D$ is the positive definite matrix to improve system dynamics, and $\hat{\boldsymbol{H}}(\boldsymbol{\theta})$, $\hat{\boldsymbol{F}}$, and $\hat{\boldsymbol{G}}(\boldsymbol{\theta})$ are estimated compensation matrixes for $\boldsymbol{H}(\boldsymbol{\theta})$, $\boldsymbol{F}$, and $\boldsymbol{G}(\boldsymbol{\theta})$, respectively. All of the estimated values in $\hat{\boldsymbol{H}}(\boldsymbol{\theta})$, $\hat{\boldsymbol{F}}$, and $\hat{\boldsymbol{G}}(\boldsymbol{\theta})$ are obtained by a series of calibration tests.

The joint positions of typical motions between four basic states are recorded and gathered *via* a series of trials, utilizing the designed torque compensation control. As a result of acquisition and procession, reference motion positions of the actuated joints are obtained and presented in Fig. 5. Regarding the joint positions of knee and hip, vertical direction is selected as initial position (0), and the flexion of hip and knee are the positive direction. The procedures of standing up and sitting down are reverse. Meanwhile, during these procedures, bilateral leg motions are the same. As an example, the first step and stop are left leg swing and right leg swing respectively in the Fig. 5. During walking procedure, bilateral leg motions are alternate circulation. Meanwhile, the knee position varies between 0° and 50°, and the hip position varies between −20° and 20° in one period. The overall trend of reference positions are reliable[29,30].

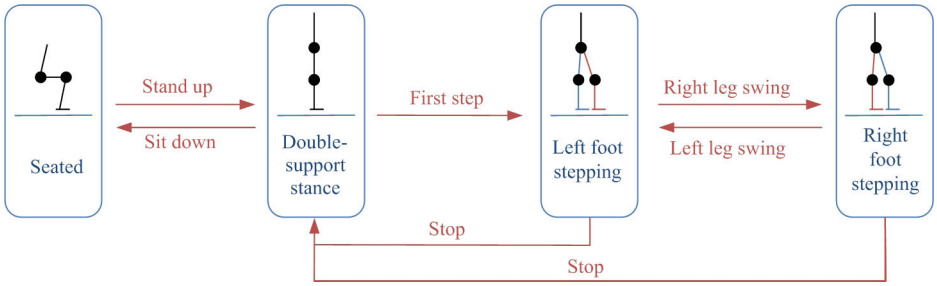

Fig. 4 The state machine: four basic states and transitions between states.

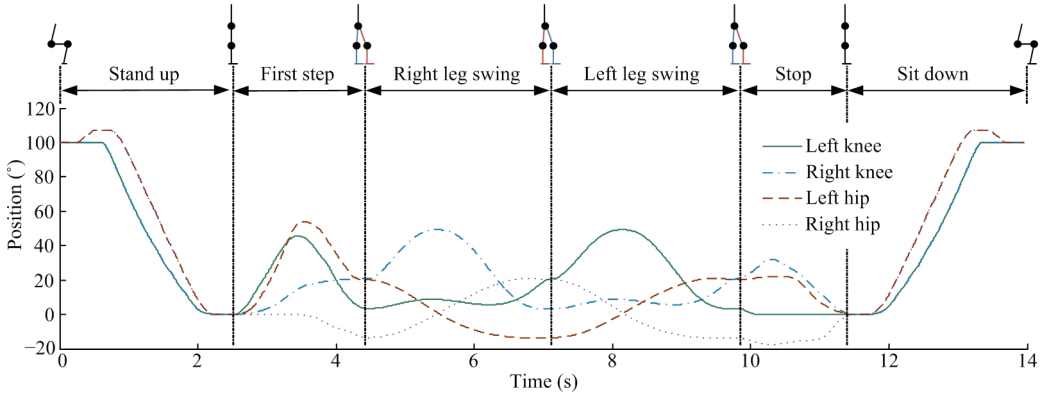

Fig. 5 Reference motion positions of the joints.

3.3 Online parameterization method

Importing the reference motion positions of joints as shown in Fig. 5 into the control system, gait control based on the state machine can be realized. However, the invariant gait is lack of adaptability and practicality. Thus, we propose a parametric gait online control method *via* three parameters, which are velocity, step-length, and step-height.

Linear interpolation method is utilized in the velocity control of gait, and i_v is defined as the velocity coefficient parameter. The control period of the exoskeleton system is 5 ms. Assume the reference position array of motion is $\boldsymbol{P}[\Theta]$ and the number of the position data is Θ. Meanwhile, the changed position array of motion is $\boldsymbol{P}_N[i_v\Theta]$, and the number of the changed position data is $i_v\Theta$. Therefore, the velocity changes to $1/i_v$ multiple of the origin. Assume an arbitrary position value of the $\boldsymbol{P}_N[i_v\Theta]$ is $P_N(i)$ and it can be expressed as:

$$\begin{aligned} P_N(i)=&P(\text{floor}(i/i_v))+(P(\text{floor}(i/i_v)+1)\\ &-P(\text{floor}(i/i_v)))\times(i/i_v-\text{floor}(i/i_v)), \end{aligned} \tag{3}$$

where floor(i/i_v) is the integer part of i/i_v.

Fig. 6 shows different curves of knee positions in the swing phase when i_v varies from 0.5 to 1.5. The swing phase spends 1.34 s, 2.67 s, and 4.01 s, respectively, when i_v is 0.5, 1.0, and 1.5. The motion time is proportional with i_v. Therefore, a series of joint positions with different motion velocities can be real-time generated by adjusting i_v, utilizing the above method.

Step-length and step-height can be utilized to describe the foot trajectory of a gait period. Kinematics models including Eqs. (4) and (5) is established and employed for the transformation between joint positions and their corresponding foot trajectory. i_l and i_h are defined as the coefficient parameters of step-length and step-height, respectively. Under Cartesian Coordinates, the hip position in the sagittal plane is selected as the coordinate origin. (x, z) represents the foot trajectory. θ_1 and θ_2 represent the motion joint positions of hip and knee, respectively. l_1 and l_2 represent the lengths of thigh and shank, respectively. Meanwhile, l_1 = 410 mm and l_2 = 480 mm. Then,

$$\begin{cases} x=l_1\sin\theta_1+l_2\sin(\theta_1-\theta_2)\\ z=l_1\cos\theta_1+l_2\cos(\theta_1-\theta_2),\\ h=l_1+l_2-z \end{cases} \tag{4}$$

Therefore, the foot trajectory can be described by (x, h). The reference motion positions of joints in the Fig. 5

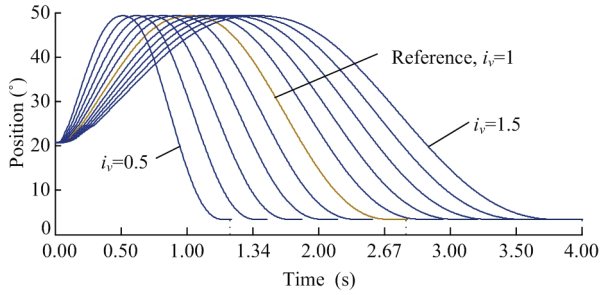

Fig. 6 Different knee position curves in swing phase when i_v varies from 0.5 to 1.5 (variation unit is 0.1).

can be transformed into the reference foot trajectory (x_0, h_0), as shown in Fig. 7. Let $x = i_l x_0$, $h = i_h h_0$. Thus, a series of foot trajectories can be real-time generated by adjusting i_l and i_h. Fig. 7 shows the different foot trajectories when i_l varies from 0.6 to 1.4 and i_h synchronously varies from 0.4 to 2.0. Therefore, the step-length and step-height are proportional with i_l and i_h, respectively.

The changed joint positions can be transformed from the foot trajectory correspondingly, by means of inverse kinematics model, as:

$$\begin{cases} \theta_2 = \arccos\left(\dfrac{x^2 + z^2 - (l_1^2 + l_2^2)}{2 l_1 l_2}\right) \\ \theta_1 = \arcsin \dfrac{x}{\sqrt{(l_1 + l_2\cos\theta_2)^2 + (l_2 \sin\theta_2)^2}} \\ \qquad + \arctan \dfrac{l_2 \sin\theta_2}{l_1 + l_2 \cos\theta_2} \end{cases}, \quad (5)$$

Let $i_l = 1.1$ and $i_h = 1.3$, the generated knee position curve in the swing phase is shown in Fig. 8. Its starting point and stopping point are changed compared with the reference position curve. Therefore, the data will lead to discontinuous, if the step-length or step-height of the next step is changed. The numerical approximation

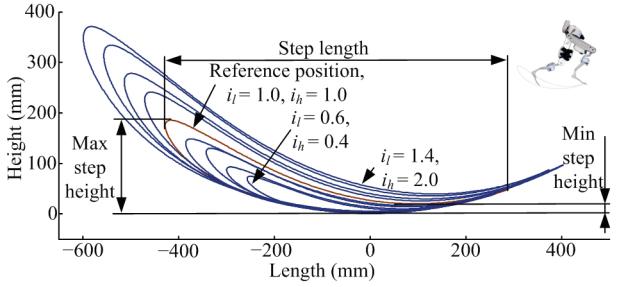

Fig. 7 Different foot trajectories when i_l varies from 0.6 to 1.4 (variation unit is 0.1).

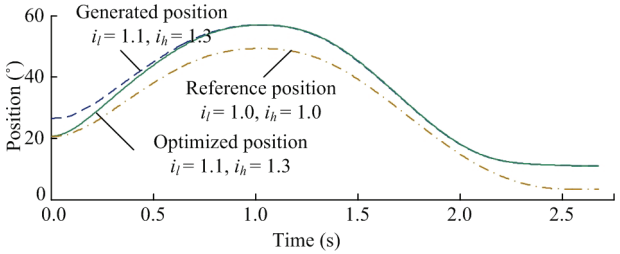

Fig. 8 Reference, generated, and optimized knee position curves in swing phase.

method is employed to optimize the generated position, in order to guarantee that the step-length and step-height of every single step could be changed continuously. Assume the reference position array is $\boldsymbol{P}_R[\Theta]$ and the number of the position data is Θ. The generated position array which is changed i_l and i_h is $\boldsymbol{P}_G[\Theta]$. And, the optimized position array is $\boldsymbol{P}_O[\Theta]$. Thus,

$$\begin{cases} P_O(1) = P_R(1) \\ P_O(i) = P_O(i-1) + \dfrac{P_G(i) - P_O(i-1)}{\Theta} \times i \quad (2 \le i \le \Theta) \end{cases}, \quad (6)$$

According to Eq. (6), the optimized position array can be obtained, and the optimized position curve of knee in the swing phase is also shown in Fig. 8. The overall trend of the optimized curve is similar with the generated curve. Meanwhile, the step-length and step-height of every step can be changed independently and smoothly.

Obviously, i_h is related with i_l. After adjusting i_l and i_h, there are two principles to guarantee the realization of the generated positions. (a) Eq. (5) has the real solutions, (b) $-30 \le \theta_1 \le 120$ and $0 \le \theta_2 \le 150$. By means of calculation and calibration, the boundary values of i_l and i_h are shown in Fig. 9. Thus, the ranges of i_l and i_h should be between the two curves in the Fig. 9.

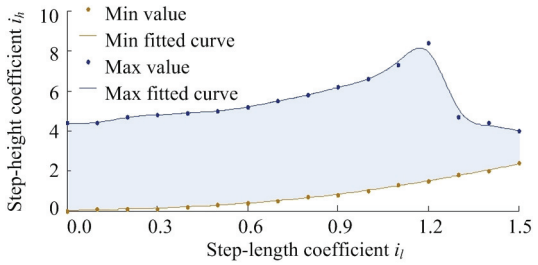

Fig. 9 Boundary values of i_l and i_h (accuracy is 0.1).

4 Tests and results

In order to test and verify the parametric gait online generation approach proposed in this paper, two walking tests on flat terrain are performed. In the two tests, three subjects are healthy males (average 173 cm, 62 kg).

Fig. 10 illustrates the setup of the experimental equipment. The handle is employed to manipulate the exoskeleton wirelessly, for servo and transitions between the basic states. A CANalyst is utilized to translate the information of joint motions. Moreover, a pressure sensor based on the Hall effect principle is designed and employed to adjust the gait parameters conveniently. In this pressure sensor, a magnet (ϕ 6 mm × 2 mm) and a Hall sensor (SS49E) are installed in a cantilever structure. Meanwhile, the output voltage proportionally varies with the pressure. In addition, the mapping relationships between the output and the gait parameters can be defined by the user. In this paper, the predefined rule is that the parameter values of velocity, step-length, and step-height vary with the output value of pressure sensor proportionally.

Two tests are performed with each repeated three times in this paper. In the test case 1, there are two kinds of steps, that is, short-quick step (i_l = 0.9, i_h = 0.9, and i_v = 0.8) and long-slow step (i_l = 1.2, i_h = 1.5, and i_v = 1.2). In the starting state, left leg is in the stance phase, and right leg is in the swing phase. In addition, short-quick step and long-slow step appear in the stance phase and swing phase alternately every three steps. In the test case 2, there are four kinds of steps, that is, (i_l = 0.9, i_h = 0.9, and i_v = 0.8), (i_l = 1.0, i_h = 1.1, and i_v = 1.0), (i_l =1.1, i_h =1.3, and i_v = 1.1), and (i_l = 1.2, i_h = 1.5, and i_v = 1.2). Every step varies from short-quick step to long-slow step and back to short-quick step again. Variety appears in every step within stance phase or swing phase, which is different with the test case 1. Similarly, the right leg within the starting state is in the swing phase. The joint positions are gathered and the foot trajectories are calculated, as shown in the Figs. 11 and 12. In addition, some key features of the gait with different parameters in these tests are obtained and presented in Table 1.

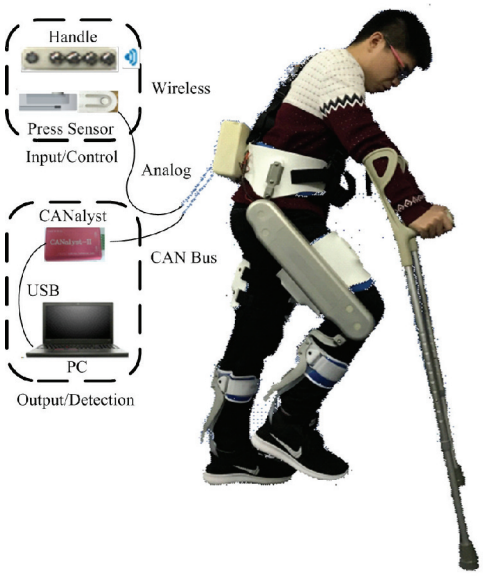

Fig. 10 Tests of parametric gait online generation.

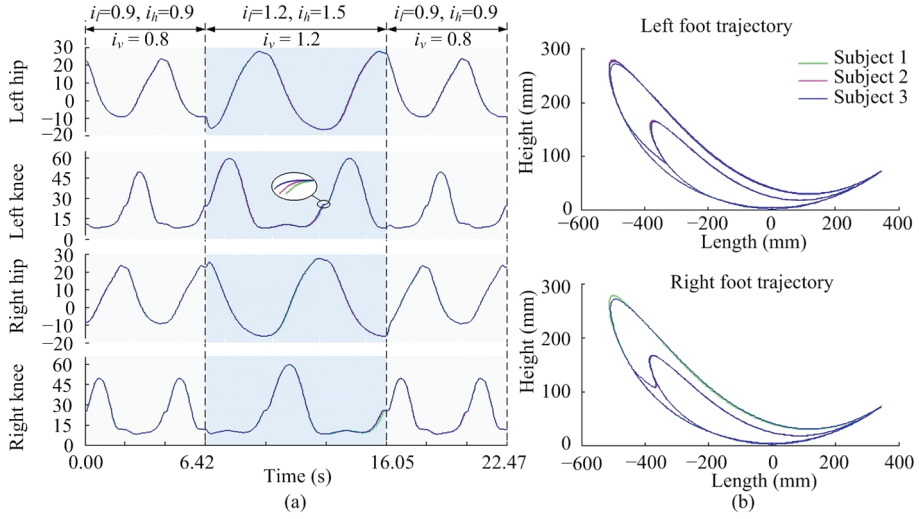

Fig. 11 Test case 1: short-quick step and long-slow step alternate every three steps. (a) Joint positions of bilateral hip and knee (unit: degree); (b) feet trajectories.

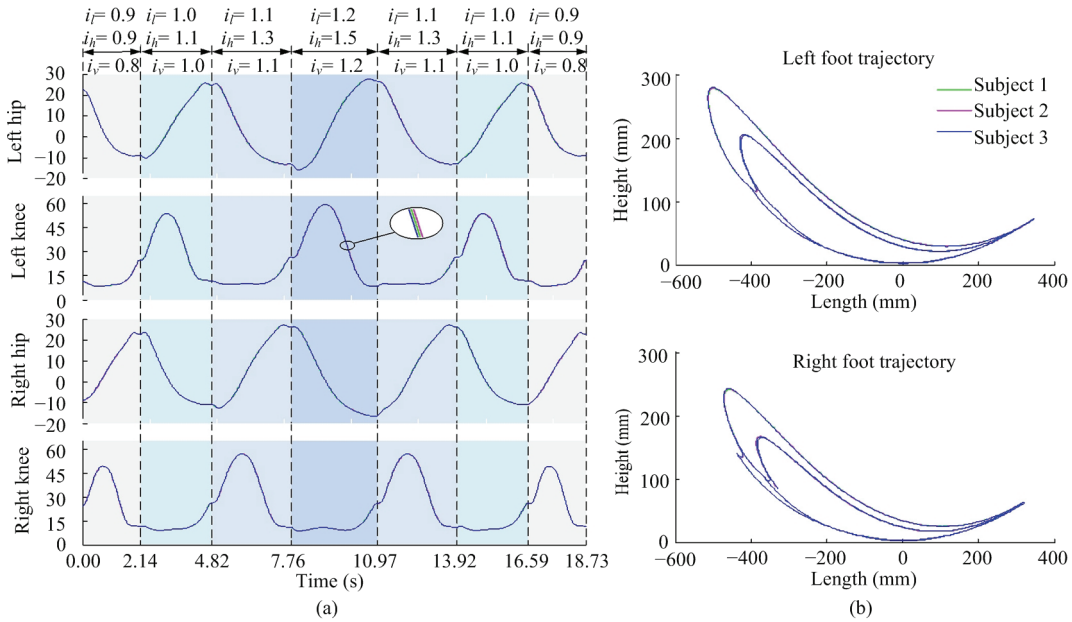

Fig. 12 Test case 2: every step varies from short-quick step to long-slow step and back to short-quick step again. (a) joint positions of bilateral hip and knee (unit: degree); (b) feet trajectories.

Table 1 Key features of gait with different parameters

Gait parameters	Period of one step	Hip position in SwP		Hip position in StP		Knee position in SwP		Knee position in StP	
		Max value	Min value	Max value	Min value	Max value	Min value	Max value	Min value
$i_l = 0.9$, $i_h = 0.9$, and $i_v = 0.8$	2.14 s	23°	−9°	23°	−9°	50°	11°	25°	8°
$i_l = 1.0$, $i_h = 1.1$, and $i_v = 1.0$	2.68 s	25°	−11°	25°	−11°	53°	12°	26°	9°
$i_l = 1.1$, $i_h = 1.3$, and $i_v = 1.1$	2.95 s	26°	−13°	26°	−13°	57°	11°	26°	9°
$i_l = 1.2$, $i_h = 1.5$, and $i_v = 1.2$	3.21 s	28°	−16°	28°	−16°	59°	9°	26°	9°

SwP: swing phase; StP: stance phase.
All of the maximum and minimum position values in this table are average values of a set of test values.

According to the results of these tests, the gait trajectories of three subjects are basically identical. In addition, the joint position errors between the three trajectories are less than 1°. The period of one step is proportional to i_v. The range and the peak values of hip positions are proportional to i_l and i_h. Meanwhile, the maximum value of knee positions in the swing phase is proportional to i_l and i_h. These mean the user needs to swing the thigh and shank more to achieve a larger step. The minimum value of knee positions in the swing phase is almost invariable except the scenario with $i_l = 1.2$ and $i_h = 1.5$. The user needs more knee extension for a larger step before landing the foot, whereas knee would be in a comfortable position when the step fits him. The motions of knee in the stance phase are not varied significantly to adapt to different steps. In these tests, user walks with the assistant of crutches, the user's knee does not achieve the full extension. Therefore, the minimum value of knee positions is 8°. The motions of the bilateral legs are consistent. However, the differences between the feet trajectories which are shown in Figs. 11 and 12 are owing to the different transitions between the swing phase and stance phase.

As shown in Figs. 11 and 12, the generated curves of every step are smooth and rational before and after the transition. Meanwhile, the curves of the joint positions and their corresponding foot trajectories are consistent. In conclusion, the online generation of gait and the changeability of every step are tested and verified.

5 Conclusion

In this paper, a novel modular lower-limb exoskeleton for individuals with paraplegia is developed. Meanwhile, a convenient and effective approach of gait online generation is proposed for the exoskeleton. Based on the state machine, this approach combines a para-

metric gait control method with the torque compensation control strategy, in order to obtain reliable and well-directed source data. By means of the proposed approach, the parametric gait is realized and two test cases are performed *via* controlling the parameters of velocity, step-length, and step-height. The results demonstrate that parametric gait can be online generated and every step is varied smoothly and correctly. Effectiveness and practicability of the gait online generation method proposed in this paper are validated. In our future work, the authors will focus on the tests and evaluations of this method on paraplegics.

Acknowledgment

This work is supported by the National Key R&D Program of China (Grant 2017YFB1302301), and the Joint Research Fund (U1613219) between the National Nature Science Foundation of China (NSFC) and Shen Zhen.

References

[1] Thuret S, Moon L D F, Gage F H. Therapeutic interventions after spinal cord injury. *Nature Reviews Neuroscience*, 2006, **7**, 628–643.

[2] Anderson K D. Targeting recovery: Priorities of the spinal cord-injured population. *Journal of Neurotrauma*, 2004, **21**, 1371–1383.

[3] Eng J J, Levins S M, Townson A F, Mah-Jones D, Bremner J, Huston G. Use of prolonged standing for individuals with spinal cord injuries. *Physical Therapy*, 2001, **81**, 1392–1399.

[4] Young A J, Ferris D P. State of the art and future directions for lower limb robotic exoskeletons. *IEEE Transactions on Neural Systems and Rehabilitation Engineering*, 2017, **25**, 171–182.

[5] Esquenazi A, Talaty M, Jayaraman A. Powered exoskeletons for walking assistance in persons with central nervous system injuries: A narrative review. *PM&R*, 2017, **9**, 46–62.

[6] He Y, Eguren D, Luu T P, Contreras-Vidal J L. Risk management and regulations for lower limb medical exoskeletons: A review. *Medical Devices*, 2017, **10**, 89–107.

[7] Contreras-Vidal J L, Bhagat N A, Brantley J, Cruz-Garza J G, He Y T, Manley Q, Nakagome S, Nathan K, Tan S H, Zhu F S. Powered exoskeletons for bipedal locomotion after spinal cord injury. *Journal of Neural Engineering*, 2016, **13**, 031001.

[8] Yan T F, Cempini M, Oddo C M, Vitiello N. Review of assistive strategies in powered lower-limb orthoses and exoskeletons. *Robotics and Autonomous Systems*, 2015, **64**, 120–136.

[9] Arazpour M, Hutchins S W, Ahmadi Bani M. The efficacy of powered orthoses on walking in persons with paraplegia. *Prosthetics and Orthotics International*, 2015, **39**, 90–99.

[10] Gwynne P. Technology: Mobility machines. *Nature*, 2013, **503**, S16–S17.

[11] Dollar A M, Herr H. Lower extremity exoskeletons and active orthoses: Challenges and state-of-the-art. *IEEE Transactions on Robotics*, 2008, **24**, 144–158.

[12] Long Y, Du Z J, Chen C F, Wang W D, He L, Mao X W, Xu G Q, Zhao G Y, Li X Q, Dong W. Development and analysis of an electrically actuated lower extremity assistive exoskeleton. *Journal of Bionic Engineering*, 2017, **14**, 272–283.

[13] Zeilig G, Weingarden H, Zwecker M, Dudkiewicz I, Bloch A, Esquenazi A. Safety and tolerance of the ReWalk™ exoskeleton suit for ambulation by people with complete spinal cord injury: A pilot study. *The Journal of Spinal Cord Medicine*, 2012, **35**, 96–101.

[14] Talaty M, Esquenazi A, Briceno J E. Differentiating ability in users of the ReWalk™ powered exoskeleton: An analysis of walking kinematics. *Proceedings of IEEE* 13*th International Conference on Rehabilitation Robotics* (*ICORR*), Seattle, USA, 2013, 1–5.

[15] Strausser K A, Swift T A, Zoss A B, Kazerooni H, Bennett B C. Mobile exoskeleton for spinal cord injury: Development and testing. *Proceedings of ASME Dynamic Systems and Control Conference*, Arlington, USA, 2011, 419–425.

[16] Strausser K A, Kazerooni H. The development and testing of a human machine interface for a mobile medical exoskeleton. *Proceedings of IEEE/RSJ International Conference on Intelligent Robots and Systems* (*IROS*), San Francisco, USA, 2011, 4911–4916.

[17] Farris R J, Quintero H A, Murray S A, Ha K H, Hartigan C, Goldfarb M. A preliminary assessment of legged mobility provided by a lower limb exoskeleton for persons with paraplegia. *IEEE Transactions on Neural Systems and Rehabilitation Engineering*, 2014, **22**, 482–490.

[18] Farris R J, Quintero H A, Goldfarb M. Preliminary evaluation of a powered lower limb orthosis to aid walking in paraplegic individuals. *IEEE Transactions on Neural Systems and Rehabilitation Engineering*, 2011, **19**, 652–659.

[19] Quintero H, Farris R, Hartigan C, Clesson I, Goldfarb M. A powered lower limb orthosis for providing legged mobility in paraplegic individuals. *Topics in Spinal Cord Injury Re-*

habilitation, 2011, **17**, 25–33.

[20] Quintero H A, Farris R J, Goldfarb M. A method for the autonomous control of lower limb exoskeletons for persons with paraplegia. *Journal of Medical Devices*, 2012, **6**, 0410031–0410036.

[21] Murray S, Goldfarb M. Towards the use of a lower limb exoskeleton for locomotion assistance in individuals with neuromuscular locomotor deficits. *Proceedings of Annual International Conference of Engineering in Medicine and Biology Society* (*EMBC*), San Diego, USA, 2012, 1912–1915.

[22] Tsukahara A, Hasegawa Y, Eguchi K, Sankai Y. Restoration of gait for spinal cord injury patients using HAL with intention estimator for preferable swing speed. *IEEE Transactions on Neural Systems and Rehabilitation Engineering*, 2015, **23**, 308–318.

[23] Hassan M, Kadone H, Suzuki K, Sankai Y. Wearable gait measurement system with an instrumented cane for exoskeleton control. *Sensors*, 2014, **14**, 1705–1722.

[24] Kawamoto H, Taal S, Niniss H, Hayashi T, Kamibayashi K, Eguchi K, Sankai Y. Voluntary motion support control of robot suit HAL triggered by bioelectrical signal for hemiplegia. *Proceedings of Annual International Conference of Engineering in Medicine and Biology Society* (*EMBC*), Buenos Aires, Argentina, 2010, 462–466.

[25] Suzuki K, Mito G, Kawamoto H, Hasegawa Y, Sankai Y. Intention-based walking support for paraplegia patients with robot suit HAL. *Advanced Robotics*, 2007, **21**, 1441–1469.

[26] Lamin H, Laribi M A, Bennour S, Romdhane L, Zeghloul S. Design study of a cable-based gait training machine. *Journal of Bionic Engineering*, 2017, **14**, 232–244.

[27] Zhang S, Wang C, Wu X, Liao Y, Wang P, Cai S. Four-legged gait planning method for a mobile medical exoskeleton with a pair of crutches. *Proceedings of IEEE International Conference on Information and Automation* (*ICIA*), Lijiang, China, 2015, 631–636.

[28] Bai S, Low K H. Terrain evaluation and its application to path planning for walking machines. *Advanced Robotics*, 2001, **15**, 729–748.

[29] Linskell J. CGA Normative Gait Database, [2018-04-25], http://www.clinicalgaitanalysis.com/data/index.html

[30] Winter D A. *Biomechanics and Motor Control of Human Movement*, 4*th* ed, John Wiley & Sons, Hoboken, USA, 2009, 341–345.